PAPER

# Bit Error Rate Analysis of OFDM with Pilot-Assisted Channel Estimation

**Richol KU**[†], **Shinsuke TAKAOKA**[†], ***Student Members***, ***and*** **Fumiyuki ADACHI**[†a)], ***Member***

**SUMMARY** The objective of this paper is to develop the theoretical foundation to the pilot-assisted channel estimation using delay-time domain windowing for the coherent detection of OFDM signals. The pilot-assisted channel estimation using delay-time domain windowing is jointly used with polynomial interpolation, decision feedback and Wiener filter. A closed-form BER expression is derived. The impacts of the delay-time domain window width, multipath channel decay factor, the maximum Doppler frequency are discussed. The theoretical analysis is confirmed by computer simulation.

***key words:*** *OFDM, channel estimation, impulse response, polynomial interpolation, decision feedback, Wiener filter*

## 1. Introduction

The next generation mobile communication systems must support very high-speed data services. On the other hand, the channels in these system will be severely frequency-selective [1]. As a transmission method, orthogonal frequency division multiplexing (OFDM) has been attracting attention since it can avoid the inter-symbol interference (ISI) [2], [3]. An accurate channel estimation technique is necessary for the coherent detection of OFDM signals. The pilot-assisted channel estimation [4], [5] using delay-time domain windowing [6] is promising. To improve the tracking ability against the time variation of the fading, the delay-time domain channel estimation can be jointly used with polynomial interpolation [7], decision feedback [8] and Wiener filtering [9]. So far, the bit error rate (BER) performance achievable with the pilot-assisted channel estimation jointly using delay-time domain windowing and polynomial interpolation, decision feedback or Wiener filtering was evaluated by computer simulation only, and there has been no theoretical analysis.

The Objective of this paper is to develop the theoretical foundation of the pilot-assisted channel estimation using delay-time domain windowing. We derive the theoretical BER expressions so as to predict the average BER performance, without resorting to the computer simulation, in a frequency-selective fading channel. The remainder of this paper is organized as follows. The transmission system model of OFDM is presented in Sect. 2. Channel estimation using delay-time domain windowing jointly used with polynomial interpolation, decision feedback and Wiener filter is described in Sect. 3. The BER analysis is presented and the closed-form BER expression is derived in Sect. 4. In Sect. 5, the theoretical and computer simulated BER performances are presented to confirm the theoretical analysis. The paper is concluded in Sect. 6.

Manuscript received March 27, 2006.
Manuscript revised December 5, 2006.

[†]The authors are with Tohoku University, Sendai-shi, 980-8579 Japan.
a) E-mail: adachi@ecei.tohoku.ac.jp

DOI: 10.1093/ietcom/e90–b.7.1725

## 2. OFDM Transmission System Model

The OFDM transmitter/receiver structure is illustrated in Fig. 1. $N_c$-subcarrier OFDM is assumed. In a transmitter, the binary data sequence is transformed into data-modulated symbol sequence. Then a known pilot sequence of $N_c$ symbols $\{d^n_{0,k};\ k = 0 \sim N_c - 1\}$ is periodically inserted into every $(M-1)\times N_c$ data symbols $\{d^n_{m,k};\ m = 1 \sim M - 1,\ k = 0 \sim N_c - 1\}$ for the $n$th frame. The pilot-inserted symbol sequence is serial-to-parallel (S/P) converted into $N_c$ parallel streams for generating the OFDM signal by $N_c$-point IFFT. Finally, the cyclic prefix of $N_g$ samples is inserted at the beginning of each OFDM symbol as the GI before transmission. One pilot OFDM symbol and its following $(M-1)$ data OFDM symbols constitute one frame, as shown in Fig. 2.

The equivalent baseband representation of the $m$th OFDM symbol in the $n$th frame is given by

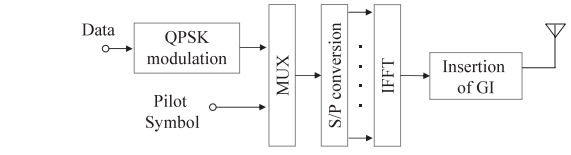


(a) Transmitter.

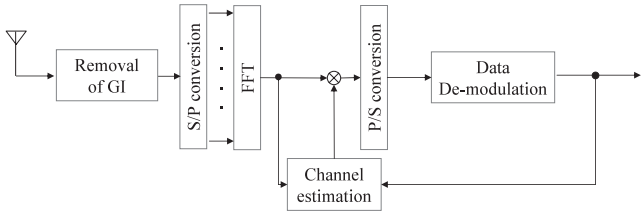


(b) Receiver.

**Fig. 1** OFDM transmitter/receiver structure.

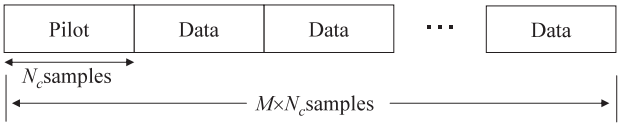


**Fig. 2** Frame structure.

$$s_m^n(t) = \sqrt{2S}\sum_{k=0}^{N_c-1} d_{m,k}^n \exp\left(j2\pi k\frac{t}{N_c}\right), \quad (1)$$

where $S$ denotes the signal power per subcarrier. The OFDM signal is transmitted via an $L$-path frequency-selective fading channel. Assuming block-fading, the channel impulse response for the reception of the $m$th OFDM symbol in the $n$th frame can be represented as [10]

$$h_m^n(\tau) = \sum_{l=0}^{L-1} h_{m,l}^n \delta(\tau - \tau_l), \quad (2)$$

where $h_{m,l}^n$ and $\tau_l$ are the path gain and delay-time of the $l$th path, respectively and $\delta(t)$ is the delta function. The maximum delay-time is assumed to be shorter than $N_g$ samples. The channel has an exponential power delay profile and $\{h_{m,l};\ m = 0 \sim M-1,\ l = 0 \sim L-1\}$ are independent zero mean complex Gaussian variables with variance

$$E\left[\left|h_{m,l}^n\right|^2\right] = \frac{1-\alpha}{1-\alpha^{-L}}\alpha^{-l}, \quad (3)$$

where $\alpha$ is the decay factor and $E[\cdot]$ represents the ensemble average operation.

The received $m$th OFDM symbol in the $n$th frame can be expressed as

$$r_m^n(t) = \sum_{l=0}^{L-1} h_{m,l}^n s_m^n(t-\tau_l) + n_m^n(t), \quad (4)$$

where $n_m^n(t)$ is the additive white Gaussian noise (AWGN) with the single-sided power spectrum density $N_0$. After the removal of GI, $N_c$-point FFT is applied to obtain

$$\begin{aligned} R_{m,k}^n &= \frac{1}{N_c}\sum_{t=0}^{N_c-1} r_m^n(t)\exp\left(-j2\pi k\frac{t}{N_c}\right) \\ &= \sqrt{2S}\, d_{m,k}^n H_{m,k}^n + N_{m,k}^n, \end{aligned} \quad (5)$$

where $H_{m,k}^n$ and $N_{m,k}^n$ are the channel gain and the noise component at the $k$th subcarrier, respectively, and are given by

$$\begin{cases} H_{m,k}^n = \sum_{l=0}^{L-1} h_{m,l}^n \exp\left(-j2\pi k\frac{\tau_l}{N_c}\right) \\ N_{m,k}^n = \frac{1}{N_c}\sum_{t=0}^{N_c-1} n_m^n(t)\exp\left(-j2\pi k\frac{t}{N_c}\right) \end{cases}. \quad (6)$$

$N_{m,k}^n$ is a zero-mean complex Gaussian variable with variance $2(N_0/T_c)/N_c$, where $T_c$ is given as $T_c = T_s/(N_c+N_g)$ with $1/T_s$ is the symbol rate. Letting the estimate of $H_{m,k}^n$ be $\tilde{H}_{m,k}^n$, coherent detection of the $m$th symbol is represented as

$$\tilde{d}_{m,k}^n = R_{m,k}^n\left(\tilde{H}_{m,k}^n\right)^*. \quad (7)$$

## 3. Channel Estimation Based on Delay-Time Domain Windowing

The pilot-assisted channel estimation using delay-time domain windowing is illustrated in Fig. 3. At the beginning

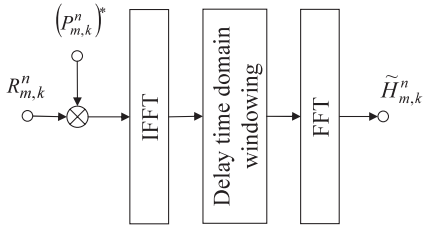


**Fig. 3** Channel estimation using delay-time domain windowing.

of each frame, the channel estimate $\hat{H}_{0,k}^n$ is obtained by removing the pilot modulation. Without loss of generality, $d_{0,k}^n$=1+$j$0 is used. $\hat{H}_{0,k}^n$ is given as

$$\hat{H}_{0,k}^n = \sqrt{2S}H_{0,k}^n + N_{0,k}^n. \quad (8)$$

$N_c$-point IFFT is applied to $\{\hat{H}_{0,k}^n;\ k = 0 \sim N_c-1\}$ to obtain $\hat{h}_0^n(\tau)$ as

$$\begin{aligned} \hat{h}_0^n(\tau) &= \sum_{k=0}^{N_c-1} \hat{H}_{0,k}^n \exp\left(j2\pi k\frac{\tau}{N_c}\right) \\ &= \sqrt{2S}\sum_{l=0}^{L-1} h_{0,l}^n \delta(\tau-\tau_l) + n_0^n(\tau), \end{aligned} \quad (9)$$

which is the noisy channel impulse response. The noise can be reduced by applying the window $w(\tau)$ to $\hat{h}_0^n(\tau)$ as

$$\tilde{h}_0^n(\tau) = \hat{h}_0^n(\tau)w(\tau), \quad (10)$$

where

$$w(\tau) = \begin{cases} 1, & 0 \le \tau < W \\ 0 & \tau \ge W \end{cases}. \quad (11)$$

where $W$ is the delay-time domain window width.

Finally, $N_c$-point FFT is applied to obtain the noise-reduced instantaneous channel gain estimate as

$$\begin{aligned} \tilde{H}_{0,k}^n &= \frac{1}{N_c}\sum_{t=0}^{W-1} \tilde{h}_0^n(\tau)\exp\left(-j2\pi k\frac{\tau}{N_c}\right) \\ &= \sqrt{2S}H_{0,k}^n + \tilde{N}_{0,k}^n, \end{aligned} \quad (12)$$

where

$$\tilde{N}_{0,k}^n = \frac{1}{N_c}\sum_{t=0}^{W-1} n_0^n(\tau)\exp\left(-j2\pi k\frac{\tau}{N_c}\right). \quad (13)$$

is a zero-mean complex Gaussian noise with variance $2(W/N_c)(N_0/T_c)/N_c$.

### 3.1 Polynomial Interpolation

For tracking against time variations of the channel gain, the polynomial interpolation [11] is considered. The channel estimate $\tilde{H}_{m,k}^n$ for coherent detection of the $m$th OFDM symbol in the $n$th frame is given by

$$\tilde{H}^n_{m,k} = \sqrt{2S}\,\bar{H}^n_{m,k} + \bar{N}^n_{m,k}$$
$$= \begin{cases} \tilde{H}^n_{0,k}, & \text{0th-order} \\ \dfrac{M-m}{M}\cdot\tilde{H}^n_{0,k} + \dfrac{m}{M}\cdot\tilde{H}^{n+1}_{0,k}, & \text{1st-order} \\ \left(1-\dfrac{m}{M}\right)\left(1-\dfrac{1}{2}\dfrac{m}{M}\right)\tilde{H}^n_{0,k} + 2\dfrac{m}{M}\left(1-\dfrac{1}{2}\dfrac{m}{M}\right)\tilde{H}^{n+1}_{0,k} \\ \quad -\dfrac{1}{2}\dfrac{m}{M}\left(1-\dfrac{m}{M}\right)\tilde{H}^{n+2}_{0,k}, & \text{2nd-order,} \end{cases} \tag{14}$$

where

$$\bar{H}^n_{m,k} = \begin{cases} H^n_{0,k}, & \text{0th-order} \\ \left(1-\dfrac{m}{M}\right)H^n_{0,k} + \dfrac{m}{M}H^{n+1}_{0,k}, & \text{1st-order} \\ \left(1-\dfrac{m}{M}\right)\left(1-\dfrac{1}{2}\dfrac{m}{M}\right)H^n_{0,k} + 2\dfrac{m}{M}\left(1-\dfrac{1}{2}\dfrac{m}{M}\right)H^{n+1}_{0,k} \\ -\dfrac{1}{2}\dfrac{m}{M}\left(1-\dfrac{m}{M}\right)\cdot H^{n+2}_{0,k}, & \text{2nd-order} \end{cases} \tag{15}$$

and

$$\bar{N}^n_{m,k} = \begin{cases} \tilde{N}^n_{0,k}, & \text{0th-order} \\ \left(1-\dfrac{m}{M}\right)\tilde{N}^n_{0,k} + \dfrac{m}{M}\tilde{N}^{n+1}_{0,k}, & \text{1st-order} \\ \left(1-\dfrac{m}{M}\right)\left(1-\dfrac{1}{2}\dfrac{m}{M}\right)\tilde{N}^n_{0,k} + 2\dfrac{m}{M}\left(1-\dfrac{1}{2}\dfrac{m}{M}\right)\tilde{N}^{n+1}_{0,k} \\ -\dfrac{1}{2}\dfrac{m}{M}\left(1-\dfrac{m}{M}\right)\tilde{N}^{n+2}_{0,k}, & \text{2nd-order.} \end{cases} \tag{16}$$

### 3.2 Decision Feedback

When the Doppler spread is getting faster, the channel estimation using interpolation becomes inaccurate. It is necessary to insert more pilot symbols to improve the tracking ability. But this results in lower transmission efficiency.

The pilot-assisted channel estimation using delay-time domain windowing can be jointly used with decision feedback as illustrated in Fig. 4. The decision result on $d^n_{m-1,k}$ is denoted by $\breve{d}^n_{m-1,k}$ and feedback to remove the data modulation from $R^n_{m-1,k}$ to obtain

$$\breve{H}^n_{m-1,k} = R^n_{m-1,k}/\breve{d}^n_{m-1,k}. \tag{17}$$

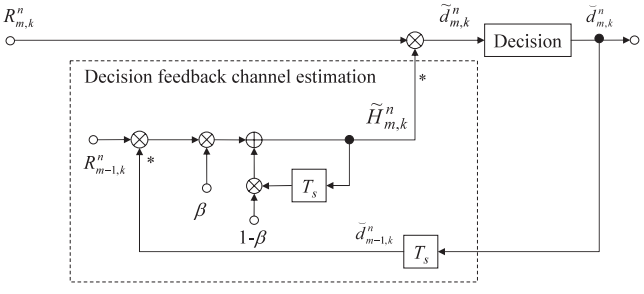


**Fig. 4** Decision feedback.

In order to reduce the noise and the error propagation due to the decision feedback, the 1st-order infinite impulse response (IIR) filter with forgetting factor $\beta$ is applied. The output $\tilde{H}^n_{m,k}$ of IIR filter is the channel gain estimate, which is given by

$$\tilde{H}^n_{m,k} = \sqrt{2S}\,\bar{H}^n_{m,k} + \bar{N}^n_{m,k} = (1-\beta)\,\tilde{H}^n_{m-1,k} + \beta\breve{H}^n_{m-1,k} \tag{18}$$

with $\breve{H}^n_{0,k} = \tilde{H}^n_{0,k}$ (which is the channel estimate obtained by delay-time domain windowing), where

$$\begin{cases} \bar{H}^n_{m,k} = (1-\beta)^m H^n_{0,k} + \beta\displaystyle\sum_{i=1}^{m}(1-\beta)^{i-1}\,H^n_{m-i,k} \\ \bar{N}^n_{m,k} = (1-\beta)^m\,\tilde{N}^n_{0,k} + \beta\displaystyle\sum_{i=1}^{m}(1-\beta)^{i-1}\,N^n_{m-i,k} \end{cases}. \tag{19}$$

### 3.3 Wiener Filter

A $Q$-order Wiener filter shown in Fig. 5 is considered. The channel estimate $\tilde{H}^n_{m,k}$ is given as

$$\tilde{H}^n_{m,k} = \sqrt{2S}\,\bar{H}^n_{m,k} + \bar{N}^n_{m,k} = \tilde{\boldsymbol{H}}^n_{0,k}\boldsymbol{W}_{m,k}, \tag{20}$$

where $\tilde{\boldsymbol{H}}^n_{0,k} = [\tilde{H}^n_{0,k}, \tilde{H}^{n+1}_{0,k}\cdots\tilde{H}^{n+Q-1}_{0,k}]$ is the estimated gain vector filtering and $\boldsymbol{W}_{m,k} = [w_{m,k}(0), \cdots, w_{m,k}(Q-1)]^T$ is the tap coefficient vector. $\bar{H}^n_{m,k}$ and $\bar{N}^n_{m,k}$ in Eq. (20) can be given as

$$\begin{cases} \bar{H}^n_{m,k} = H^n_{0,k}w_{m,k}(0) + \cdots + H^{n+(Q-1)}_{0,k}w_{m,k}(Q-1) \\ \bar{N}^n_{m,k} = \tilde{N}^n_{0,k}w_{m,k}(0) + \cdots + \tilde{N}^{n+(Q-1)}_{0,k}w_{m,k}(Q-1). \end{cases} \tag{21}$$

$\boldsymbol{W}_{m,k}$ is updated according to the minimum-mean square error (MMSE) criterion and is given by [12]

$$\boldsymbol{W}_{opt} = \left(\boldsymbol{R} + \frac{1}{SNR}\boldsymbol{I}\right)^{-1}\boldsymbol{r}, \tag{22}$$

where $\boldsymbol{I}$ is $Q \times Q$ identity matrix,

$$\boldsymbol{R} = \begin{pmatrix} R_{0,0} & \cdots & R_{0,Q-1} \\ \vdots & \ddots & \vdots \\ R_{Q-1,0} & \cdots & R_{Q-1,Q-1} \end{pmatrix},\ \boldsymbol{r} = \begin{pmatrix} r_0 \\ \vdots \\ r_{Q-1} \end{pmatrix}, \tag{23}$$

where

$$\begin{cases} R_{p,q} = E\left[H^{n+p}_{0,k}H^{n+q^*}_{0,k}\right] \text{ for } p,q = 0 \sim Q-1 \\ r_q = E\left[H^n_{m,k}H^{n+q^*}_{0,k}\right] \end{cases}. \tag{24}$$

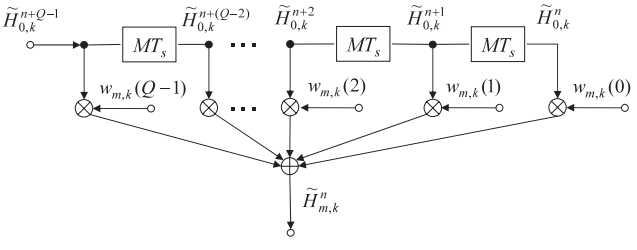


**Fig. 5** Wiener filter.

## 4. BER Analysis

The quadrature-phase shift keying (QPSK) is assumed for data modulation. Coherent detection for the QPSK data symbol $d_{m,k}^n$ is carried out as $\tilde{d}_{m,k}^n = R_{m,k}^n \left(\tilde{H}_{m,k}^n\right)^*$ (see Eq. (7)). Assuming a Rayleigh fading channel, $R_{m,k}^n$ and $\tilde{H}_{m,k}^n$ are zero-mean complex Gaussian variables for the given $d_{m,k}^n$. Without loss of generality, we assume $d_{m,k}^n = (1 + j) / \sqrt{2}$. The average BER is obtained from

$$\begin{aligned} P_{4b,m} &= \text{Prob}\left[\text{Re}\left[R_{m,k}^n \left(\tilde{H}_{m,k}^n\right)^*\right] < 0\right] \\ &= \text{Prob}\left[\text{Re}\left[XY^*\right] < 0\right] \end{aligned} \tag{25}$$

with $X = R_{m,k}^n$ and $Y = \tilde{H}_{m,k}^n$. Remember that $\text{Re}\left[XY^*\right]$ is a special case of the general quadratic form [13, Eq. (4B.1)] defined as $A|X|^2 + B|Y|^2 + CXY^* + C^*X^*Y$ with $A = B$=0 and $C$=1/2. Following Ref. [13, Appendix 4B], the average BER for $d_{m,k}^n$ can be derived as (its derivation is omitted for the sake of brevity)

$$\begin{aligned} P_{4b,m} &= \text{Prob}\left[\text{Re}\left[R_{m,k}^n \left(\tilde{H}_{m,k}^n\right)^*\right] < 0\right] \\ &= \frac{1}{2}\left[1 - \frac{\text{Re}[\mu_m]}{\sqrt{1 - \text{Im}^2[\mu_m]}}\right], \end{aligned} \tag{26}$$

where $\mu_m$ is the normalized covariance and is given by

$$\mu_m = \frac{\mu_{xy,m}}{\sqrt{\mu_{xx,m}\mu_{yy,m}}} \tag{27}$$

with

$$\begin{cases} \mu_{xx,m} = E\left[\left|R_{m,k}^n\right|^2\right], \quad \mu_{yy,m} = E\left[\left|\tilde{H}_{m,k}^n\right|^2\right], \\ \mu_{xy,m} = E\left[R_{m,k}^n \left(\tilde{H}_{m,k}^n\right)^*\right] \end{cases}. \tag{28}$$

Since

$$E\left[\left|N_{0,k}^n\right|^2\right] = 2\frac{N_0}{T_c} \cdot \frac{1}{N_c},\ E\left[N_{m,k}^n \cdot \bar{N}_{0,k}^{n^*}\right] = 0, \tag{29}$$

we have

$$\begin{cases} \mu_{xx,m} = 2S + 2\dfrac{N_0}{T_c} \cdot \dfrac{1}{N_c},\ \mu_{yy,m} = 2S\,(A_1 + A_2), \\ \mu_{xy,m} = 2S \cdot A_3 \cdot \left(\dfrac{1+j}{\sqrt{2}}\right) \end{cases} \tag{30}$$

with

$$\begin{cases} A_1 = E\left[\left|\bar{H}_{m,k}^n\right|^2\right], \quad A_2 = \dfrac{1}{2S}E\left[\left|\bar{N}_{m,k}^n\right|^2\right], \\ A_3 = E\left[H_{m,k}^n \cdot \left(\bar{H}_{m,k}^n\right)^*\right] \end{cases}. \tag{31}$$

Therefore, $\mu_m$ of Eq. (27) can be given as

$$\mu_m = \frac{A_3}{\sqrt{\left(1 + \dfrac{1}{2}\left(\dfrac{E_b}{N_0}\right)^{-1}\right)(A_1 + A_2)}}\left(\frac{1+j}{\sqrt{2}}\right), \tag{32}$$

where $E_b/N_0$ (= $0.5(S \cdot T_c \cdot N_c)/N_0$) denotes the signal energy per bit-to-AWGN power spectrum density ratio. Finally, we obtain the following general BER expression:

$$\begin{aligned} &P_{4b,m} \\ &= \frac{1}{2}\left[1 - \frac{\text{Re}[A_3] - \text{Im}[A_3]}{\sqrt{\begin{matrix} 2\left(1 + \dfrac{1}{2}\left(\dfrac{E_b}{N_0}\right)^{-1}\right)(A_1 + A_2) - |A_3|^2 \\ -2\text{Re}[A_3]\text{Im}[A_3] \end{matrix}}}\right]. \end{aligned} \tag{33}$$

The average BER can be obtained by averaging Eq. (33) over a frame as

$$P_{4b} = \frac{1}{(M-1)}\sum_{m=1}^{M-1} P_{4b,m}. \tag{34}$$

In the following, we obtain $A_1$, $A_2$ and $A_3$ for delay-time domain windowing, interpolation, decision edback and Wiener filtering. We assume the Jake's fading model [1] for each propagation path.

(1) Polynomial Interpolation

First, we consider the 0th order interpolation. In this case, delay-time domain windowing is only used. We have $\tilde{H}_{m,k}^n = \tilde{H}_{0,k}^n$ for $m = 1 \sim M-1$ and therefore, $A_1$, $A_2$ and $A_3$ are given by

$$\begin{cases} A_1 = \dfrac{1 - \alpha^{-(l_{\max}+1)}}{1 - \alpha^{-L}} \\ A_2 = \dfrac{1}{2}\left(\dfrac{E_b}{N_0}\right)^{-1}\left(\dfrac{W}{N_c}\right) \\ A_3 = J_0\left(2\pi m f_D T_s\right)\dfrac{1 - \alpha^{-(l_{\max}+1)}}{1 - \alpha^{-L}} \end{cases} \quad \text{for the 0th-order interpolation,} \tag{35}$$

where $l_{\max} = \arg\max_l\{\tau_l < N_g\}$, $J_0(x)$ is the 0th-order Bessel function of the first kind and $T_s$ is the OFDM symbol duration equal to $T_s = (N_c + W)T_c$. Substituting Eq. (35) into Eq. (33), we have

$$\begin{aligned} &P_{4b,m} \\ &= \frac{1}{2}\left[1 - \frac{J_0\left(2\pi m f_D T_s\right)}{\sqrt{\begin{matrix} 2\left\{\dfrac{1 - \alpha^{-(l_{\max}+1)}}{1 - \alpha^{-L}}\right\}^{-1}\left\{1 + \dfrac{1}{2}\left(\dfrac{E_b}{N_0}\right)^{-1}\right\} \\ \left\{1 + \dfrac{1}{2}\left(\dfrac{1 - \alpha^{-(l_{\max}+1)}}{1 - \alpha^{-L}}\right)^{-1}\left(\dfrac{E_b}{N_0}\right)^{-1}\left(\dfrac{W}{N_c}\right)\right\} \\ -J_0\left(2\pi m f_D T_s\right)^2 \end{matrix}}}\right]. \end{aligned} \tag{36}$$

For $E_b/N_0 \gg 1$, the average BER can be approximated as

$$P_{4b,m} = \frac{1}{2}\left[1 - \frac{J_0\left(2\pi f_D T_s \cdot m\right)}{\sqrt{\begin{matrix} 2A\left\{1 + \dfrac{1}{2}A\left(\dfrac{E_b}{N_0}\right)^{-1}\left(\dfrac{W}{N_c}\right)\right\} \\ -J_0\left(2\pi f_D T_s \cdot m\right)^2 \end{matrix}}}\right]. \tag{37}$$

When $E_b/N_0 \to \infty$, Eq. (37) reduces to

$$P_{4b,m} = \frac{1}{2}\left[1 - \frac{J_0\left(2\pi f_D T_s \cdot m\right)}{\sqrt{2A - J_0\left(2\pi f_D T_s \cdot m\right)^2}}\right]. \tag{38}$$

Next, $A_1$, $A_2$ and $A_3$ for the 1st and 2nd-order interpolations are given as

$$\begin{cases} A_1 = \left(\dfrac{1-\alpha^{-(l_{\max}+1)}}{1-\alpha^{-L}}\right)\left[\left(1-\dfrac{m}{M}\right)^2 + 2\left(\dfrac{m}{M}\right)\left(1-\dfrac{m}{M}\right) \right. \\ \quad \left. \times J_0\left(2\pi M f_D T_s\right) + \left(\dfrac{m}{M}\right)^2\right] \\ A_2 = \dfrac{1}{2}\left(\dfrac{E_b}{N_0}\right)^{-1}\left(\dfrac{W}{N_c}\right)\left[\left(\dfrac{m}{M}\right)^2 + \left(1-\dfrac{m}{M}\right)^2\right] \\ A_3 = \left(\dfrac{1-\alpha^{-(l_{\max}+1)}}{1-\alpha^{-L}}\right)\left[\left(1-\dfrac{m}{M}\right) J_0\left(2\pi m f_D T_s\right) \right. \\ \quad \left. + \left(\dfrac{m}{M}\right) J_0\left(2\pi M\left(1-\dfrac{m}{M}\right) f_D T_s\right)\right] \\ \qquad \text{for 1st-order interpolation.} \end{cases} \tag{39}$$

and

$$\begin{cases} A_1 = \left(\dfrac{1-\alpha^{-(l_{\max}+1)}}{1-\alpha^{-L}}\right) \times \left[4\dfrac{m}{M}\left(1-\dfrac{1}{2}\dfrac{m}{M}\right)\left(1-\dfrac{m}{M}\right)^2 \right. \\ \quad \times \begin{pmatrix} 2J_0\left(2\pi M f_D T_s\right) \\ -\dfrac{1}{2}J_0\left(2\pi M f_D T_s\right) \end{pmatrix} + \left\{\left(1-\dfrac{1}{2}\dfrac{m}{M}\right)\left(1-\dfrac{m}{M}\right)\right\}^2 \\ \quad \left. + \left\{2\dfrac{m}{M}\left(1-\dfrac{1}{2}\dfrac{m}{M}\right)\right\}^2 + \left\{\dfrac{1}{2}\dfrac{m}{M}\left(1-\dfrac{m}{M}\right)\right\}^2\right] \\ A_2 = \dfrac{1}{2}\left(\dfrac{E_b}{N_0}\right)^{-1}\left(\dfrac{W}{N_c}\right)\left[\left\{\left(1-\dfrac{1}{2}\dfrac{m}{M}\right)\left(1-\dfrac{m}{M}\right)\right\}^2 \right. \\ \quad \left. + \left\{2\dfrac{m}{M}\left(1-\dfrac{1}{2}\dfrac{m}{M}\right)\right\}^2 + \left\{\dfrac{1}{2}\dfrac{m}{M}\left(1-\dfrac{m}{M}\right)\right\}^2\right] \\ A_3 = \left(\dfrac{1-\alpha^{-(l_{\max}+1)}}{1-\alpha^{-L}}\right)\left\{\left(1-\dfrac{1}{2}\dfrac{m}{M}\right)\left(1-\dfrac{m}{M}\right) J_0\left(2\pi m f_D T_s\right) \right. \\ \quad + 2\dfrac{m}{M}\left(1-\dfrac{1}{2}\dfrac{m}{M}\right) J_0\left(2\pi M\left(1-\dfrac{m}{M}\right) f_D T_s\right) \\ \quad \left. + \dfrac{1}{2}\dfrac{m}{M}\left(1-\dfrac{m}{M}\right) J_0\left(2\pi M\left(2-\dfrac{m}{M}\right) f_D T_s\right)\right\} \\ \qquad \text{for 2nd-order interpolation.} \end{cases} \tag{40}$$

(2) Decision Feedback

We assume ideal decision feedback, i.e., no error propagation is considered. $A_1$, $A_2$ and $A_3$ for ideal decision feedback are given as

$$\begin{cases} A_1 = \left(\dfrac{1-\alpha^{-(l_{\max}+1)}}{1-\alpha^{-L}}\right)\left\{2\beta(1-\beta)^m \sum_{i=1}^{m}(1-\beta)^{i-1} \right. \\ \quad \left. \times J_0\left(2\pi f_D T_s (m-i)\right) + (1-\beta)^{2m} + \beta^2 A_4\right\} \\ A_2 = \dfrac{1}{2}\left(\dfrac{E_b}{N_0}\right)^{-1}\left[\left(\dfrac{W}{N_c}\right)(1-\beta)^{2m} + \beta^2\dfrac{1-(1-\beta)^{2m}}{1-(1-\beta)^2}\right] \\ A_3 = \left(\dfrac{1-\alpha^{-(l_{\max}+1)}}{1-\alpha^{-L}}\right)\left\{(1-\beta)^m J_0\left(2\pi f_D T_s \cdot m\right) \right. \\ \quad \left. + \beta\sum_{i=1}^{m}(1-\beta)^{i-1} J_0\left(2\pi f_D T_s i\right)\right\} \end{cases} \tag{41}$$

where

$$\begin{aligned} A_4 &= E\left[\left|\sum_{i=1}^{m} H_{m-i,k}\,(1-\beta)^{i-1}\right|^2\right] \\ &= \frac{1-(1-\beta)^{2m}}{1-(1-\beta)^2} + 2\sum_{x=1}^{m-1}\frac{1-(1-\beta)^{2(m-x)}}{1-(1-\beta)^2} \\ &\quad \times (1-\beta)^x J_0\left(2\pi f_D T_s x\right). \end{aligned} \tag{42}$$

(3) Wiener Filter

We consider $Q = 1 \sim$ 3-tap Wiener filter. $A_1$, $A_2$ and $A_3$ for Wiener filter are given as

$$\begin{cases} A_1 = \left(\dfrac{1-\alpha^{-(l_{\max}+1)}}{1-\alpha^{-L}}\right)\left|w_{m,k}(0)\right|^2 \\ A_2 = \dfrac{1}{2}\left(\dfrac{E_b}{N_0}\right)^{-1}\left(\dfrac{W}{N_c}\right)\left|w_{m,k}(0)\right|^2 \\ A_3 = \left(\dfrac{1-\alpha^{-(l_{\max}+1)}}{1-\alpha^{-L}}\right) w^*_{m,k}(0) J_0\left(2\pi m f_D T_s\right) \\ \qquad \text{for } Q\text{=1,} \end{cases} \tag{43}$$

$$\begin{cases} A_1 = \left(\dfrac{1-\alpha^{-(l_{\max}+1)}}{1-\alpha^{-L}}\right)\left(\left|w_{m,k}(0)\right|^2 + \left|w_{m,k}(1)\right|^2\right) \\ \quad + 2\mathrm{Re}\left[w_{m,k}(0) w^*_{m,k}(1) J_0\left(2\pi M f_D T_s\right)\right] \\ A_2 = \dfrac{1}{2}\left(\dfrac{E_b}{N_0}\right)^{-1}\left(\dfrac{W}{N_c}\right)\left(\left|w_{m,k}(0)\right|^2 + \left|w_{m,k}(1)\right|^2\right) \\ A_3 = \left(\dfrac{1-\alpha^{-(l_{\max}+1)}}{1-\alpha^{-L}}\right)\left[w^*_{m,k}(0) J_0\left(2\pi m f_D T_s\right) \right. \\ \quad \left. + w^*_{m,k}(1) J_0\left(2\pi M f_D T_s\left(1-\dfrac{m}{M}\right)\right)\right] \\ \qquad \text{for } Q\text{=2,} \end{cases} \tag{44}$$

and

$$\begin{cases} A_1 = \left(\dfrac{1-\alpha^{-(l_{\max}+1)}}{1-\alpha^{-L}}\right)\left(\left|w_{m,k}(0)\right|^2+\left|w_{m,k}(1)\right|^2+\left|w_{m,k}(2)\right|^2\right) \\ \quad +2\mathrm{Re}\Big[w_{m,k}(0)w^*_{m,k}(1)J_0(2\pi M f_D T_s) \\ \quad +w_{m,k}(1)w^*_{m,k}(2)J_0(2\pi M f_D T_s)\Big] \\ \quad +w_{m,k}(0)w^*_{m,k}(2)J_0(4\pi M f_D T_s) \\ A_2 = \dfrac{1}{2}\left(\dfrac{E_b}{N_0}\right)^{-1}\left(\dfrac{W}{N_c}\right)\left(\left|w_{m,k}(0)\right|^2+\left|w_{m,k}(1)\right|^2+\left|w_{m,k}(2)\right|^2\right) \\ A_3 = \left(\dfrac{1-\alpha^{-(l_{\max}+1)}}{1-\alpha^{-L}}\right)\left\{w^*_{m,k}(0)J_0(2\pi f_D T_s m)\right. \\ \quad +w^*_{m,k}(1)J_0\left(2\pi M f_D T_s\left(1-\dfrac{m}{M}\right)\right) \\ \quad \left.+w^*_{m,k}(2)J_0\left(2\pi M f_D T_s\left(2-\dfrac{m}{M}\right)\right)\right\} \\ \qquad\qquad \text{for } Q=3. \end{cases} \tag{45}$$

(4) Ideal Channel Estimation

Since $A_1 = A_3 = 1$ and $A_2 = 0$, the BER is not a function of the OFDM symbol position in the frame and Eq. (34) reduces to

$$P_{4b} = \frac{1}{2}\left(1 - \frac{1}{\sqrt{1+\left(\dfrac{E_b}{N_0}\right)^{-1}}}\right). \tag{46}$$

## 5. Numerical and Simulation Results

Table 1 summarizes the numerical and simulation condition. We assume that one frame consists of 64 OFDM symbols. A sample-spaced 8-path ($L$=8) frequency-selective block Rayleigh fading channel, having an exponential power delay profile with decay factor $\alpha$, is assumed.

Figure 6 shows the average BER as a function of the delay-time domain window width when $E_b/N_0$=20 dB. A good agreement is seen between the numerical and computer simulated BERs. By reducing the window width $W$ from 255 to 29, the BER only slightly improves. The average BER can be reduced to half by using delay-time domain window having $W$=29 when $\alpha$=0 dB. However, if $W$ is set to be less than 29, the impulse response is truncated by the window and the estimated impulse response is distorted; therefore, the BER significantly increases below-$W$=29. The distortion in the estimated channel impulse is more significant for a stronger channel selectivity case (i.e., $\alpha \to 0$ dB). As a consequence, the value of $W$ can be set to the expected maximum delay time difference ($W$=29 in this paper) irrespective of the channel selectivity.

**Table 1** Numerical and simulation conditions.

| | | |
|---|---|---|
| Data modulation | | QPSK |
| No of subcarriers | | $N_c$=256 |
| GI | | $N_g$=32 |
| Channel model | Fading | $L$=8-path Rayleigh fading |
| | Power delay profile | Exponential decay profile |
| | Delay | $\tau_l$=4$l$, $l$=0~$L$−1 |
| Normalized Doppler frequency | | $f_D T_s$=0.0001~0.1 |
| Pilot insertion interval | | $M$=64 OFDM symbols |
| Delay-time domain window width | | $W$=0~$N_c$−1 |

Figure 7 shows the BER performances using 0th, 1st and 2nd-order interpolation filters as a function of the average received $E_b/N_0$ for various values of $f_D T_s$ when $L$=8 path, $\alpha$=0 dB and $W$=29. The BER performance using 0th-order interpolation greatly degrades when $f_D T_s > 0.001$ (which corresponds to a terminal moving speed higher than 40 km/h for a bit rate of 100 Mbps and 5 GHz carrier frequency) since the tracking ability of the 0th-order interpolation filter is very poor. However, the 1st and 2nd-order interpolation filters provide much better BER performance. It should be noticed that the 1st and 2nd-order interpolation filters provide almost the same BER performance. Figure 8 shows the BER performance using decision feedback with $\beta$=0.3 (we have found from computer simulation that $\beta$=0.3 can minimize the BER for $f_D T_s$=0.0001–0.01 at the average $E_b/N_0$=15 dB and also at the average $E_b/N_0$=30 dB). For perfect feedback, the BER performance is better than using interpolation filters under a fast fading environment. However, due to error propagation, the BER performance with real decision feedback degrades and becomes worse than using the 1st and 2nd-order interpolation filters.

Figure 9 shows the BER performance using Wiener filter when $\alpha$=0 dB and $L$=8. As the number of taps increases, the BER performance improves. The BER-performance of 1-tap Wiener filter and 0th-order interpolation are seen to be almost the same. The reason for this is discussed below. The causes of decision errors in the interpolation-based channel

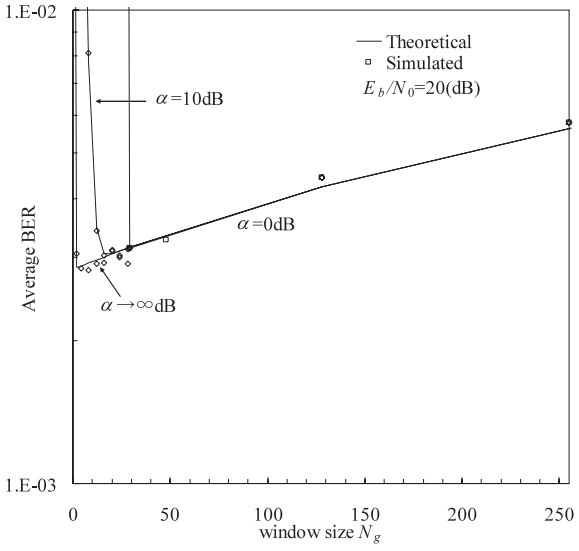


**Fig. 6** Impact of delay-time domain window width.

estimation schemes are the AWGN and the tracking error against time-variant fading. The BER due to AWGN should be the same for the 0-th order interpolation filter and the 1-tap Wiener filter, since the same delay-time domain window width is used. On the other hand, the BER floor appears in large $E_b/N_0$ region where the predominant cause of errors is the tracking error against fading. The tracking ability against fading is controlled by the tap coefficient. The tap coefficient is always 1 for the 0-th order interpolation, while it depends on the fading maximum Doppler frequency $f_D$ and the average received $E_b/N_0$ for the 1-tap Wiener filter. According to our computer simulation, the tap coefficient of the 1-tap Wiener filter was found to be 0.998 at $m$=32 (i.e., the center of a frame) when the average received $E_b/N_0$=20 dB and $f_DT_s$=0.0001. Accordingly, the tracking ability against fading is almost the same for the 0-th order interpolation and 1-tap Wiener filter, resulting in almost the same BER floor in large $E_b/N_0$ region.

The BER floor seen in large $E_b/N_0$ region depends on the tracking ability against fading. It can be seen from Fig. 7(c) and Fig. 9(c) that the 3-tap Wiener filter has a good tracking ability against fading and gives a lower BER floor than the 2nd-order interpolation when $f_DT_s < 0.008$. However, as the fading becomes too fast, e.g., $f_DT_s > 0.008$, both 3-tap Wiener filter and 2nd-order interpolation have a poor

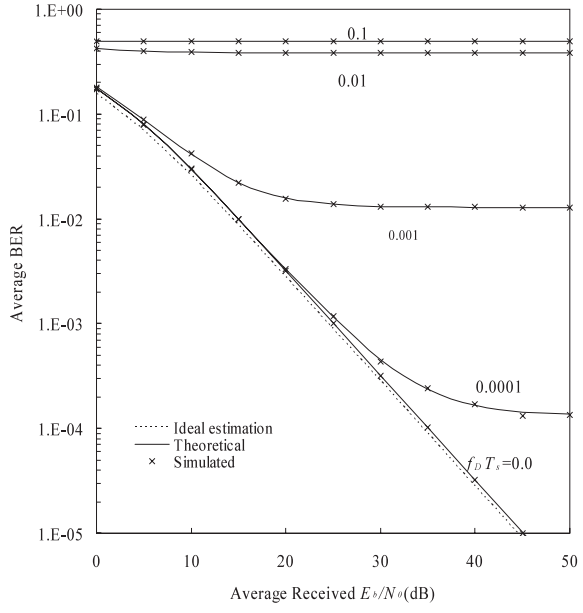


(a) 0th-order.

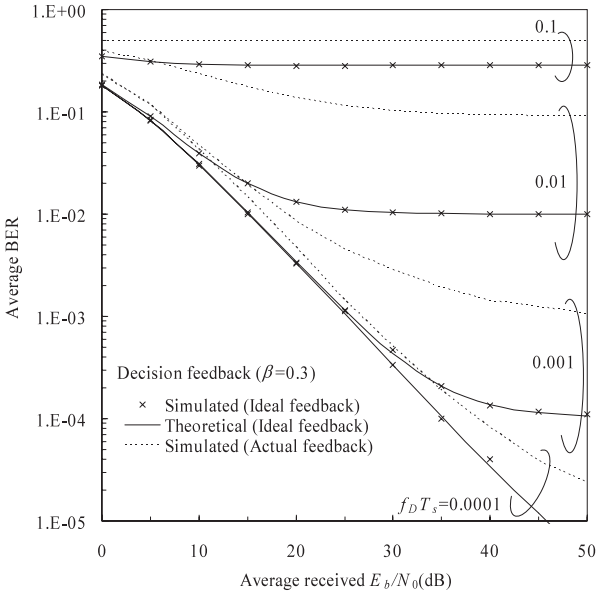


**Fig. 8** BER performance using decision feedback.

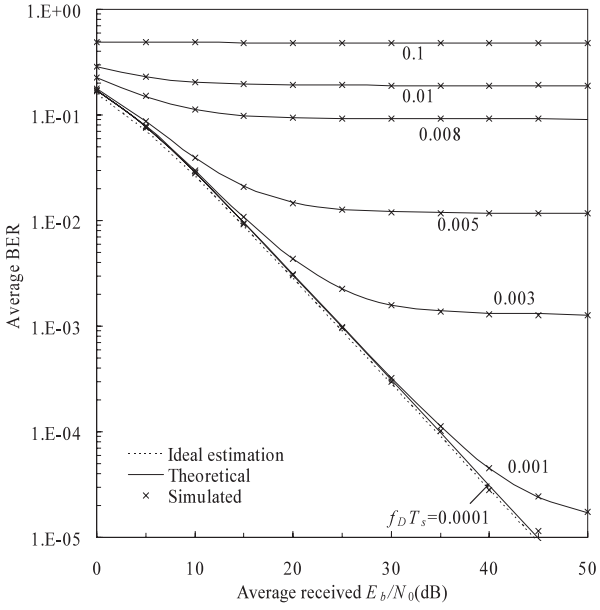


(b) 1st-order.

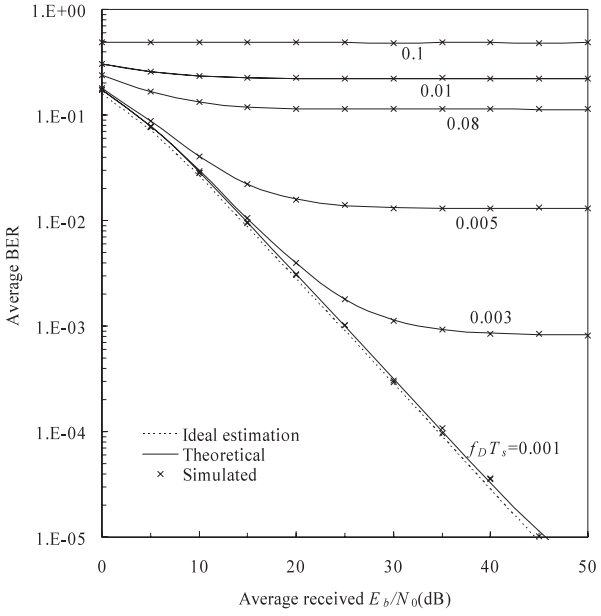


(c) 2nd-order.

**Fig. 7** BER performances using polynomial interpolation.

tracking ability against fading and yield large BER floors.

The Computer simulated BER performances are also plotted in Figs. 7–9. A fairly good agreement between the numerical and simulated BER performances is seen. This confirms our theoretical BER analysis.

## 6. Conclusion

The closed-form expression of the BER performance was derived for the pilot-assisted channel estimation using delay-time domain windowing jointly used with polynomial interpolation, decision feedback and Wiener filter. The theoretical analysis was confirmed by computer simulation. In this paper, only the uncoded case was considered. However, it is expected that even when channel coding is applied, the BER performance close to the ideal channel estimation case can be achieved due to delay-time domain windowing and decision feedback after channel decoding. The theoretical BER analysis of coded OFDM with practical channel estimation is an interesting future study.

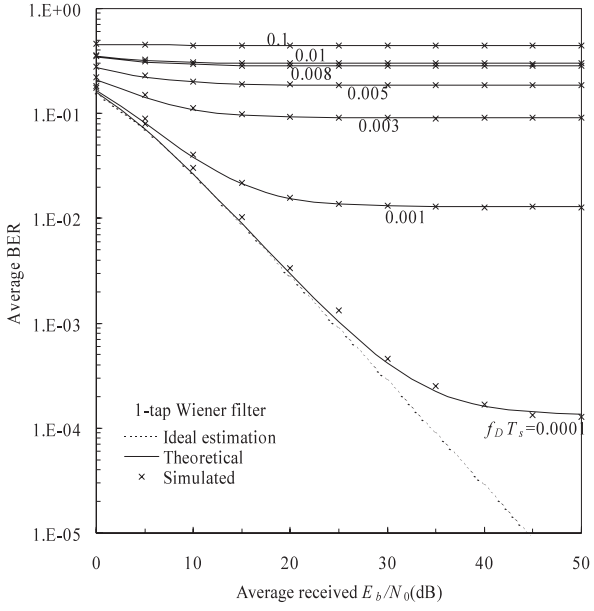


(a) 1-tap.

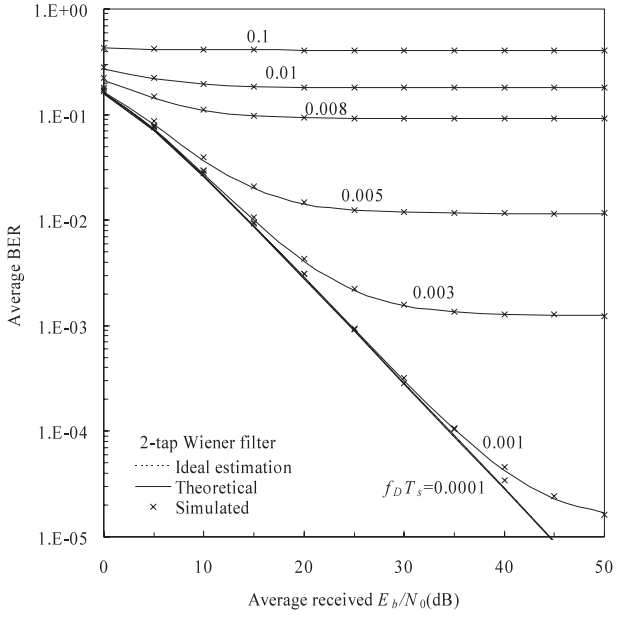


(b) 2-tap.

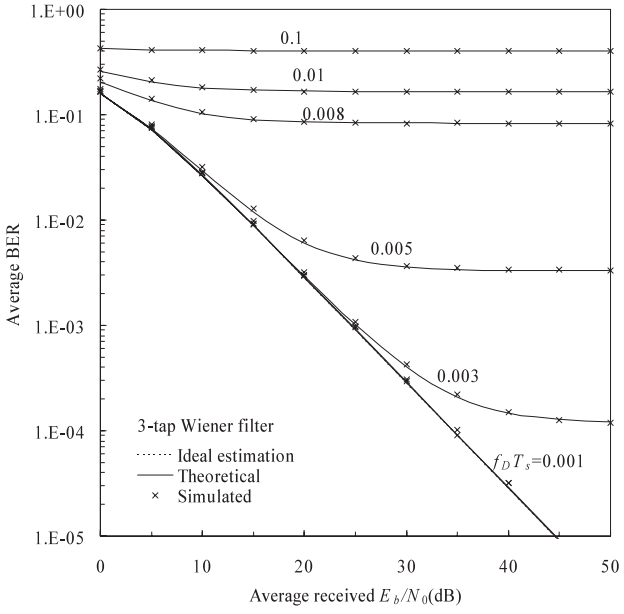


(c) 3-tap.

**Fig. 9** BER performance using Wiener filter.

### References

[1] W.C. Jakes, Jr., ed., Microwave mobile communications, Wiley, NewYork, 1974.
[2] S. Hara and R. Prasad, "Overview of multicarrier CDM," IEEE Commun. Mag., vol.35, no.12, pp.126–133, Dec. 1997.
[3] M. Okada, S. Hara, and N. Morinaga, "Bit error performance of orthogonal multicarrier modulation radio transmission system," IEICE Trans. Commun., vol.E76-B, no.2, pp.113–119, Feb. 1993.
[4] P. Hoeher, S. Kaiser, and P. Robertson, "Pilot-symbol-aided channel estimation in time and frequency," Proc. Global Telecomm. Conf. the Mini-Conf., pp.90–96, Nov. 1997.
[5] J.K. Cavers, "An analysis of pilot symbol assisted modulation for Rayleigh fading channels," IEEE Trans. Veh. Technol., vol.40, no.4, pp.686–693, Nov. 1991.
[6] J.-J. van de Beek, O. Edfors, M. Sandell, S.K. Wilson, and P.O. Borjesson, "On channel estimation in OFDM systems," IEEE Vehicular Technology Conference, vol.2, pp.815–819, July 1995.
[7] S. Sampei and T. Sunaga, "Rayleigh fading compensation for QAM in land mobile radio communications," IEEE Trans. Veh. Technol., vol.42, no.2, pp.137–147, May 1993.
[8] K. Ishihara, K. Takeda, and F. Adachi, "Decision feedback channel estimation for OFDM with STTD," Proc. 7th International Symposium on Wireless Personal Multimedia Communication (WPMC), Abano Terme, Italy, Sept. 2004.
[9] P. Hoeher, S. Kaiser, and P. Robertson, "Two-dimensional pilot-symbol-aided channel estimate on by wiener filtering," Proc. Int. Conf. Acoustics, Speech, and Signal Processing, pp.1845–1848, April 1997.
[10] S. Hara and R. Prasad, Multicarrier Techniques for 4G mobile com-

munications, Artech House, 2003.
[11] M. Abramowitz and I.A. Stegun, Handbook of mathematical functions with formulas, graphs and mathematical tables, 9th printing, Dover, New York, 1970.
[12] S. Takaoka and F. Adachi, "Pilot-assisted channel estimation using adaptive interpolation for coherent rake reception of DS-CDMA signals," Proc. 8th International Conference on Cellular and Intelligent Communications (CIC), Seoul, Korea, Oct. 2003.
[13] J.G. Proakis, Digital Communications, 3rd ed., McGraw-Hill, 1995.

**Richol Ku** received his B.S. degree in electronic and information engineering from Korea University, Tokyo, Japan, in 2003, and M.S. degree in electrical and communication engineering from Tohoku University, Sendai, Japan, in 2006. His research interests include channel estimation, especially for mobile communication systems.

**Shinsuke Takaoka** received his B.S., M.S. and Ph.D. degrees in electrical and communication engineering from Tohoku University, Sendai, Japan, in 2001, 2003 and 2006, respectively. He was a Japan Society for the Promotion of Science (JSPS) research fellow during 2003–2006. Currently, he is with Matsushita Electric Industrial Co., Ltd. His research interests include digital signal transmission techniques, especially for mobile communication systems.

**Fumiyuki Adachi** received the B.S. and Dr.Eng. degrees in electrical engineering from Tohoku University, Sendai, Japan, in 1973 and 1984, respectively. In April 1973, he joined the Electrical Communications Laboratories of Nippon Telegraph & Telephone Corporation (now NTT) and conducted various types of research related to digital cellular mobile communications. From July 1992 to December 1999, he was with NTT Mobile Communications Network, Inc. (now NTT DoCoMo, Inc.), where he led a research group on wideband/broadband CDMA wireless access for IMT-2000 and beyond. Since January 2000, he has been with Tohoku University, Sendai, Japan, where he is a Professor of Electrical and Communication Engineering at the Graduate School of Engineering. His research interests are in CDMA wireless access techniques, equalization, transmit/receive antenna diversity, MIMO, adaptive transmission, and channel coding, with particular application to broadband wireless communications systems. From October 1984 to September 1985, he was a United Kingdom SERC Visiting Research Fellow in the Department of Electrical Engineering and Electronics at Liverpool University. Dr. Adachi served as a Guest Editor of IEEE JSAC on Broadband Wireless Techniques, October 1999, Wideband CDMA I, August 2000, Wideband CDMA II, Jan. 2001, and Next Generation CDMA Technologies, Jan. 2006. He is an IEEE Fellow and was a co-recipient of the IEEE Vehicular Technology Transactions Best Paper of the Year Award 1980 and again 1990 and also a recipient of Avant Garde award 2000. He was a recipient of IEICE Achievement Award 2002 and a co-recipient of the IEICE Transactions Best Paper of the Year Award 1996 and again 1998. He was a recipient of Thomson Scientific Research Front Award 2004.